

Controlling paths of high-order harmonic generation by orthogonal two-color fields*

Ze-Hui Ma(马泽慧)^{1,2}, Cai-Ping Zhang(张彩萍)^{1,2,†}, Jun-Lin Ma(马俊琳)^{1,2}, and Xiang-Yang Miao(苗向阳)^{1,2,‡}

¹College of Physics and Information Engineering, Shanxi Normal University, Linfen 041004, China

²Key Laboratory of Spectral Measurement and Analysis of Shanxi Province, Shanxi Normal University, Linfen 041004, China

(Received 25 December 2019; revised manuscript received 13 January 2020; accepted manuscript online 30 January 2020)

Controlling paths of high-order harmonic generation from H_2^+ is theoretically investigated by numerically solving the time-dependent Schrödinger equation based on the Born–Oppenheimer approximation in orthogonal two-color fields. Our simulations show that the change of harmonic emission paths is dependent on time-dependent distribution of electrons. Compared with one-dimensional linearly polarized long wavelength laser, multiple returns are suppressed and short paths are dominant in the process of harmonic emission by two-dimensional orthogonal $\omega/2\omega$ laser fields. Furthermore, not only are multiple returns weakened, but also the harmonic emission varies from twice to once in an optical cycle by orthogonal $\omega/1.5\omega$ laser fields. Combining the time–frequency distributions and the time-dependent electron wave packets probability density, the mechanism of controlling paths is further explained. As a result, a 68-as isolated attosecond pulse is obtained by superposing a proper range of the harmonics.

Keywords: high-order harmonic generation, orthogonal two-color fields, attosecond pulse generation

PACS: 32.80.Rm, 42.65.Re, 42.65.Ky

DOI: 10.1088/1674-1056/ab7189

1. Introduction

Attosecond pulses^[1,2] have attracted a lot of attention experimentally and theoretically, and it is widely used in studying electron dynamics and detecting the internal structure of atoms, molecules, and solids. Moreover, the attosecond pulses can be synthesized from high-order harmonics^[3,4] which are emitted by the interaction of strong laser with atoms,^[5,6] molecules,^[7–9] and solids.^[10–13] The electron dynamics in harmonic generation from the atom and the small molecule with single electron are extensively investigated in one-dimensional (1D) laser field. But 1D linearly polarized light restricts the electron motion essentially to the light polarization plane where recollisions and harmonic emission occur nearly continuously over the laser pulse duration. The two-dimensional (2D) laser fields offer more possibilities for detecting the internal structure of molecules and studying the physical mechanism. At present, the 2D orthogonal fields have attracted a lot of attention.^[14–17] With orthogonally polarized two-color laser fields, Chen *et al.* researched temporal properties of high-order harmonic generation (HHG) from aligned molecules in orthogonal two-color laser fields^[18] and probed the degrees of orientation of the nonlinear polyatomic molecules via odd and even harmonics.^[19] He *et al.* studied HHG from H_2^+ in the orthogonal two-color pulses composed of strong fundamental frequency pulse and weak

direct-current pulse, and found that the harmonics in the direction of weak direct-current pulse presented pure even harmonics, while those in the direction of strong fundamental frequency presented pure odd harmonics.^[20] Gonzalez-ferez *et al.* proved that perpendicularly polarized two-color laser fields can be used to achieve stronger molecular orientation.^[21] Lu *et al.* enabled the tomographic imaging of molecular orbital with single-shot measurement in the experiment by 2D processing of electron motion in the orthogonal fields.^[22] 2D orthogonal fields can be used not only to detect molecular structure information and imaging information but also to control the paths of harmonic emission. The HHG is contributed by different trajectories, such as long and short paths, the interference between them is not conducive to synthesizing attosecond pulses. Many ways have been explored to synthesize attosecond pulses in the 1D linearly polarized laser field, such as few-cycle pulse^[23] and the two-color scheme,^[24] *etc.* Compared with the 1D laser field, the 2D orthogonal fields provide more possibilities to obtain the shorter and higher intensity attosecond pulses.

In this paper, we theoretically investigate the paths control of HHG from H_2^+ by numerically solving the Born–Oppenheimer (BO) time-dependent Schrödinger equation (TDSE). The results show that short paths are predominant while the long quantum paths are suppressed in the case of the

*Project supported by the National Natural Science Foundation of China (Grant Nos. 11974229, 11404204, and 11947002), the Scientific and Technological Innovation Program of Higher Education Institutions in Shanxi Province, China (Grant No. 2019L0468), the Natural Science Foundation for Young Scientists of Shanxi Province, China (Grant No. 201901D211404), and the Innovation Project for Postgraduates of Shanxi Province, China (Grant No. 2019SY310).

†Corresponding author. E-mail: cpzhang880822@163.com

‡Corresponding author. E-mail: sxxymiao@126.com

2D orthogonal $\omega/2\omega$ fields. Moreover, the harmonic emission paths change from twice to once in an optical cycle (o.c.) in the case of the 2D orthogonal $\omega/1.5\omega$ fields. This paper provides a simple and convenient method to control the harmonic emission paths, which can provide theoretical guidance for experiments.

2. Theoretical method

We assume that the fundamental field is linearly polarized along x axis, and the additional n -harmonic field along the y axis. With the molecular axis along the x axis, the 2D TDSE can be written as^[25–28]

$$i \frac{\partial}{\partial t} \psi(\mathbf{r}, t) = H(\mathbf{r}, t) \psi(\mathbf{r}, t). \quad (1)$$

Then, the Hamiltonian of the model molecule H_2^+ can be written as

$$H(\mathbf{r}, t) = \mathbf{p}^2/2 + V(\mathbf{r}) + \mathbf{E}(t) \cdot \mathbf{r}, \quad (2)$$

(in atomic units of $\hbar = e = m_e = 1$). In the above expression, $V(\mathbf{r})$ represents the Coulomb potential of the molecule which can be expressed as

$$V(\mathbf{r}) = -Z/(\zeta + r_1^2)^{1/2} - Z/(\zeta + r_2^2)^{1/2}, \quad (3)$$

with $r_1^2 = (x + R/2)^2 + y^2$ and $r_2^2 = (x - R/2)^2 + y^2$ in 2D cases. Here, $R = 2$ a.u. is the internuclear separation and Z is the effective nuclear charge. $\zeta = 0.5$ is the smoothing parameter which is used to avoid the Coulomb singularity. We use a grid size of $L_x \times L_y = 400$ a.u. \times 250 a.u. with a grid spacing of $\Delta x = \Delta y = 0.4$ a.u. for the x and y axes, respectively. With the above parameters, the ground-state ionization potential of H_2^+ is 1.1 a.u. The electric field of 2D orthogonal fields can be written as

$$\mathbf{E}(t) = E_x(t)\mathbf{e}_x + E_y(t)\mathbf{e}_y, \quad (4)$$

where $E_x(t) = E_0 \sin(\omega_0 t)$ and $E_y(t) = E_1 \sin(n\omega_0 t)$. E_0 (E_1) is the maximal amplitude of electric field $E_x(t)$ ($E_y(t)$). ω_0 is the laser frequency of $E_x(t)$ lasting 5 o.c. Equation (1) is solved by the second-order split-operator method.^[29] Once the wave function $\Psi(t)$ is obtained, the dipole acceleration can be given by the Ehrenfest theorem^[30]

$$a(t) = \frac{d^2}{dt^2} \langle \Psi(t) | \mathbf{r} | \Psi(t) \rangle. \quad (5)$$

In order to further understand the HHG, the time–frequency distribution is given by means of the wavelet transform^[31]

$$d_\omega(t) = \int a(t') \sqrt{\omega} W[\omega(t' - t)] dt', \quad (6)$$

$$W(x) = \frac{1}{\sqrt{\tau}} e^{ix} \exp\left(\frac{-x^2}{2\tau^2}\right). \quad (7)$$

3. Results and discussion

As we all know, the narrower attosecond pulse can be obtained by wider harmonic plateau. Compared with the short wavelength, the long wavelength is easier to extend the harmonic spectrum experimentally. It is the 1D linearly polarized long wavelength laser field ($I = 5 \times 10^{14}$ W/cm², $\lambda = 1200$ nm) that is used in the paper, and corresponding the time–frequency distribution in Fig. 1. In the process of harmonic emission, there are not only first return, but also multiple returns as shown by white arrows. The underlying mechanisms of multiple returns have been explained in our previous works.^[32,33] So, it is necessary to manipulate multiple returns, which make it difficult to synthesis the isolated attosecond pulse with the long wavelength pulse.

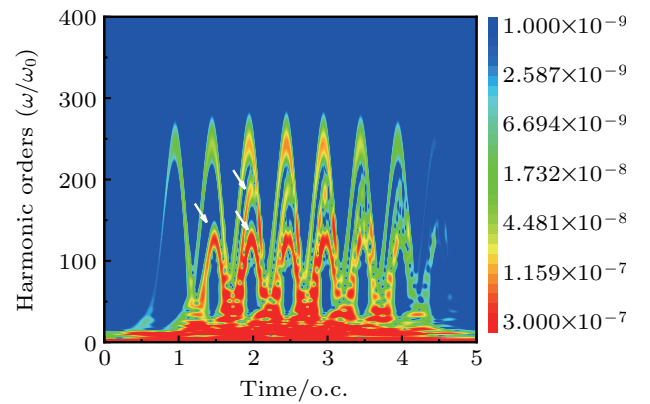


Fig. 1. Time–frequency distribution of the HHG corresponding to the case of $I = 5 \times 10^{14}$ W/cm², $\lambda = 1200$ nm in 1D linearly polarized laser field.

Multiple returns will be eliminated effectively accompanied by the suppression of the long paths.^[32] In essence, the motion time of electrons in the laser field dominates the long paths, which is mainly contributed by the early ionization and late return electrons. So the 2D orthogonal $\omega/2\omega$ field ($I_x = 5 \times 10^{14}$ W/cm², $I_y = 5 \times 10^{14}$ W/cm², $\lambda_x = 1200$ nm, $\lambda_y = 600$ nm) in Fig. 2(a) is selected, which looks like a bowknot. Here A, A', C, C' (B, D) mean the ionization (return) moments of the electrons in one cycle, the red and blue arrows mean the trend of electric field.

Obviously, the multiple returns are suppressed in the time–frequency distribution as seen in Fig. 2(b). Besides, the harmonics are emitted twice in one cycle and mainly contributed by short paths. Figures 2(c) and 2(d) show the time-dependent electron wave packets probability density of x, y axes in 0 o.c.–2 o.c., respectively. To further explore the process of harmonic emission, the results in 0 o.c.–0.5 o.c. are taken as an example. There are twice ionization around point A' (0.1 o.c.), A (0.4 o.c.), which are near the peak intensity of x, y axes in Fig. 2(a). When the electrons are ionized around point A' (0.1 o.c.), they move farther and farther from the x axis and never come back, but return around point B' (0.5 o.c.)

in y axis as shown in Figs. 2(c) and 2(d). Furthermore, when the electrons are ionized around point A (0.4 o.c.), the electrons return to the parent nucleus simultaneously in the x , y directions around point B (0.8 o.c.) in Figs. 2(c) and 2(d). Only electrons returning to the parent nucleus simultaneously in the x , y directions, will contribute to HHG. This is similar to the other twice ionization around point C' and C. Therefore, twice electron returns lead to twice harmonic emissions in one cycle.

To find the reason for suppression of multiple returns, classical computations are performed. The white lines in

Fig. 2(c) mean that the excursion of the electron trajectories in the continuum is characterized by a distance $x_0 = E_0/\omega^2$ (82 a.u.). The short trajectories cannot go beyond x_0 while the long trajectories always cross this value,^[34] moreover, the HHG is also dominated by the instantaneous electric field direction parallel to the molecules axis.^[22] As shown in the figures, the probabilities of electrons localized at the region between two white lines are overwhelming majority. It means that the long paths are weakened effectively in the process of HHG, which is consistent with Fig. 2(b).

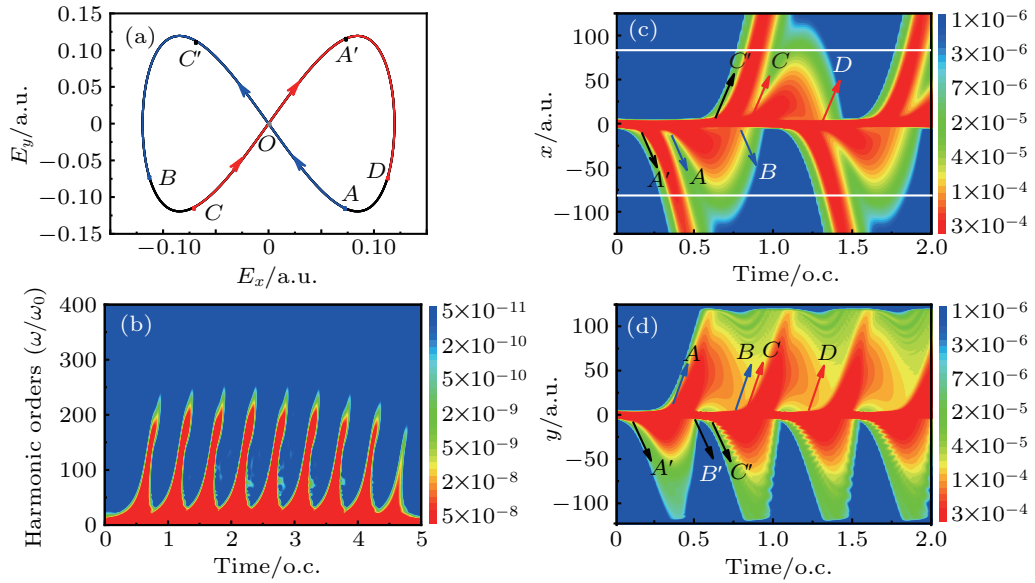


Fig. 2. (a) The sketch of the electric field of the laser pulses with the combination of $\omega/2\omega$ laser fields, $I_x = 5 \times 10^{14}$ W/cm², $I_y = 5 \times 10^{14}$ W/cm², $\lambda_x = 1200$ nm, $\lambda_y = 600$ nm. O is the origin of E_x - E_y , A, A', C, C' (B, D) mean the ionization (return) moments of the electron, the arrows represent the trend of electric field; (b) the time-frequency distribution of the HHG corresponding to the case of panel (a); (c) and (d) the time-dependent electron wave packets probability density of x , y axes, respectively. The white lines mean that the excursion of the electron trajectories in the continuum is characterized by a distance $x_0 = E_0/\omega^2$.

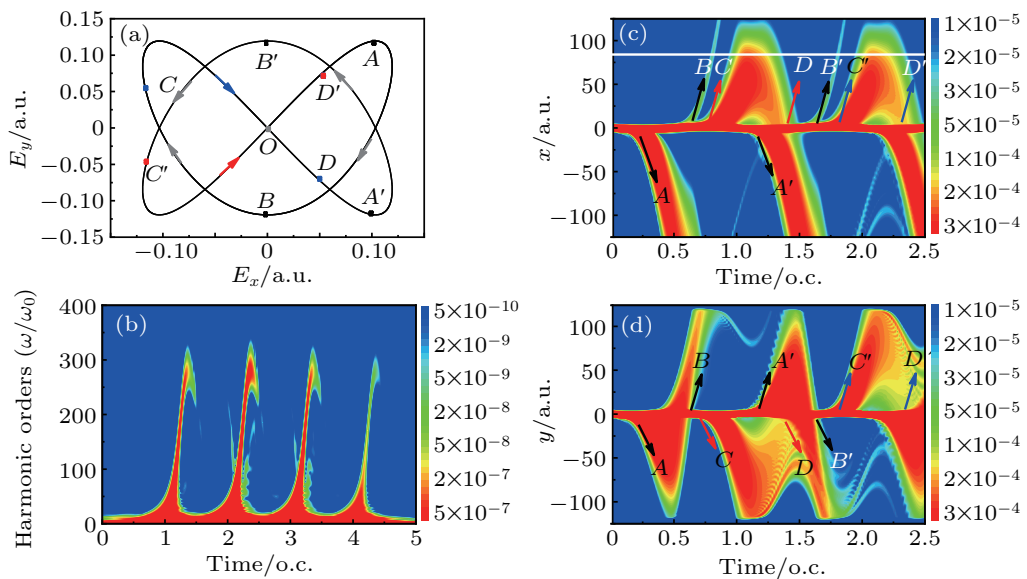


Fig. 3. (a) The electric field of the laser pulses with the combination of $\omega/1.5\omega$ laser fields in two cycles, $I_x = 5 \times 10^{14}$ W/cm², $I_y = 5 \times 10^{14}$ W/cm², $\lambda_x = 1200$ nm, $\lambda_y = 800$ nm. O is the origin of E_x - E_y , A, A', B, B', C, C' (D, D') denote the ionization (return) moments of the electron, the arrows mean the trend of electric field; (b) the time-frequency distribution of the HHG corresponding to the case of panel (a); (c) and (d) the time-dependent electron wave packets probability density of x , y axes, respectively. The white line means that classical computations show that the excursion of the electron trajectories in the continuum is characterized by a distance $x_0 = E_0/\omega^2$.

To further optimize the harmonic emission, we choose the 2D orthogonal $\omega/1.5\omega$ fields ($I_x = 5 \times 10^{14}$ W/cm², $I_y = 5 \times 10^{14}$ W/cm², $\lambda_x = 1200$ nm, $\lambda_y = 800$ nm) as displayed in Fig. 3(a), which looks like two-crossing heart. $A, A', B, B', C, C' (D, D')$ indicate the ionization (return) moments of the electron, and arrows represent the trend of electric field. The time–frequency distributions of $\omega/1.5\omega$ laser fields show that harmonic emission only once a cycle in Fig. 3(b). Figures 3(c) and 3(d) are the time-dependent electron wave packets probability densities in x, y axes in 0 o.c.–2.5 o.c. There are three ionization moments around point A (0.16 o.c.), B (0.5 o.c.), C (0.8 o.c.), respectively in one cycle. As discussed above, the harmonics are emitted once a cycle, corresponding to the process of C (0.8 o.c.) \rightarrow D (1.4 o.c.) in Figs. 3(c) and 3(d), respectively. We conclude that the harmonic emission in 2D orthogonal laser fields is strongly affected by time-dependent distribution of electrons. Furthermore, by superposing the harmonics from 120th order to 180th order, an isolated 68-as pulse is obtained as shown in Fig. 4.

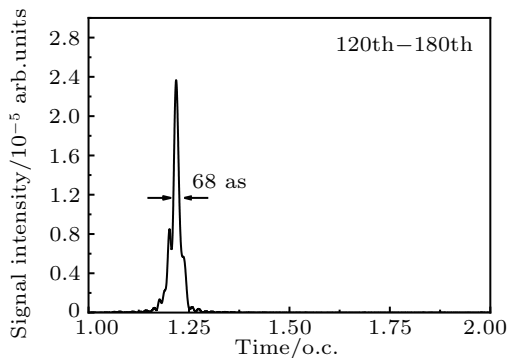


Fig. 4. The time profiles of the attosecond pulses by superposing harmonics from the 120th order to the 180th order for Fig. 3(a).

4. Conclusion

In summary, we theoretically investigated the HHG process from H_2^+ by numerically solving the Born–Oppenheimer time-dependent Schrödinger equation. We present a scheme to control paths of the harmonic emission in the orthogonal two-color fields. The results show that the harmonic is emitted twice in one cycle by the 2D orthogonal $\omega/2\omega$ laser fields, and it is mainly contributed by the short paths. Furthermore, harmonic emissions change from twice to once in one cycle by the 2D orthogonal $\omega/1.5\omega$ laser fields. In contrast, HHG from 1D linearly polarized laser field is contributed by long paths, short paths, and multiple returns. The physical mechanism of the phenomenon is explained by the time–frequency

analysis. In addition, by the time-dependent electron wave packets probability density, the law of motion of electrons in orthogonal fields is also investigated. The reason that the orthogonal two-color fields can choose the quantum paths and change the number of harmonic radiations is that the electron wave packet movement possesses different periodicities in the perpendicular direction. Moreover, an isolated 68-as pulse is directly obtained by superposing the proper range of the harmonics. Thus, our research can provide theoretical guidance for the experimental study.

References

- [1] Corkum P B and Krausz F 2007 *Nat. Phys.* **3** 381
- [2] Li P C and Chu S I 2012 *Phys. Rev. A* **86** 013411
- [3] Yuan K J and Bandrauk A D 2019 *Phys. Rev. A* **100** 033420
- [4] Milošević D B and Becker W 2002 *Phys. Rev. A* **66** 063417
- [5] L’Huillier A, Schafer K J and Kulander K C 1991 *J. Phys. B: At. Mol. Opt. Phys.* **24** 3315
- [6] Zhang J, Qi T, Pan X F, Guo J, Zhu K G and Liu X S 2019 *Chin. Phys. B* **28** 103204
- [7] Miao X Y and Zhang C P 2014 *Phys. Rev. A* **89** 033410
- [8] Li M Z, Xu Y, Jia G R and Bian X B 2019 *Phys. Rev. A* **100** 033410
- [9] Wustelt P, Oppermann F, Yue L, Möller M, Stöhlker T, Lein M, Gräfe S, Paulus G G and Saylor A M 2018 *Phys. Rev. Lett.* **121** 073203
- [10] Yu C, Jiang S C and Lu R F 2019 *Adv. Phys. X* **4** 1562982
- [11] Zuo R X, Song X H, Liu X W, Yang S D and Yang W F 2019 *Chin. Phys. B* **28** 094208
- [12] Tao Z, Chen C, Szilvasi T, Keller M, Mavrikakis M, Kapteyn H and Murnane M 2016 *Science* **353** 62
- [13] Dejean N T and Rubio A 2018 *Sci. Adv.* **4** eaao5207
- [14] Kitzler M and Lezius M 2005 *Phys. Rev. Lett.* **95** 253001
- [15] Zhang B and Lein M 2019 *Phys. Rev. A* **100** 043401
- [16] Milošević D B and Becker W 2019 *Phys. Rev. A* **100** 031401
- [17] Murakami M, Korobkin O and Horbatsch M 2013 *Phys. Rev. A* **88** 063419
- [18] Chen C, Ren D X, Han X, Yang S P and Chen Y J 2018 *Phys. Rev. A* **98** 063425
- [19] Yu S J, Li W Y, Li Y P and Chen Y J 2017 *Phys. Rev. A* **96** 013432
- [20] Xu L and He F 2019 *J. Opt. Soc. Am. B* **36** 840
- [21] Mun J H, Sakai H and González-Férez R 2019 *Phys. Rev. A* **99** 053424
- [22] Zhai C Y, Zhang X F, Zhu X S, He L X, Zhang Y F, Wang B N, Zhang Q B, Lan P F and Lu P X 2018 *Opt. Express* **3** 2775
- [23] Zhao S F, Zhou X X, Li P C and Chen Z J 2008 *Phys. Rev. A* **78** 063404
- [24] Du H C, Wang H Q and Hu B T 2010 *Phys. Rev. A* **81** 063813
- [25] Lu R F, Zhang P Y and Han K L 2008 *Phys. Rev. E* **77** 066701
- [26] Miao X Y and Zhang C P 2014 *Laser Phys. Lett.* **11** 115301
- [27] Hu J, Han K L and He G Z 2005 *Phys. Rev. Lett.* **95** 123001
- [28] Miao X Y and Du H N 2013 *Phys. Rev. A* **87** 053403
- [29] Feit M D, Fleck Jr J A and Steiger A 1982 *J. Comput. Phys.* **47** 412
- [30] Burnett K, Reed V C, Cooper J and Knight P L 1992 *Phys. Rev. A* **45** 3347
- [31] Tong X M and Chu S I 2000 *Phys. Rev. A* **61** 021802
- [32] Zhang C P, Pei Y N, Jia X F and Miao X Y 2017 *Laser Phys. Lett.* **14** 015301
- [33] Zhang C P, Xia C L, Jia X F and Miao X Y 2016 *Opt. Express* **24** 20297
- [34] Labeye M, Risoud F, Lévêque C, Caillat J, Maquet A, Shaaran T, Salières P and Taleb R 2019 *Phys. Rev. A* **99** 013412